Flooding Experiments and Modeling for Improved Reactor Safety

M. Solmos, K. J. Hogan, K. Vierow
Texas A&M University

Abstract

Countercurrent two-phase flow and "flooding" phenomena in light water reactor systems are being investigated experimentally and analytically to improve reactor safety of current and future reactors. The aspects that will be better clarified are the effects of condensation and tube inclination on flooding in large diameter tubes.

The current project aims to improve the level of understanding of flooding mechanisms and to develop an analysis model for more accurate evaluations of flooding in the pressurizer surge line of a Pressurized Water Reactor (PWR). Interest in flooding has recently increased because Countercurrent Flow Limitation (CCFL) in the AP600 pressurizer surge line can affect the vessel refill rate following a small break LOCA and because analysis of hypothetical severe accidents with the current flooding models in reactor safety codes shows that these models represent the largest uncertainty in analysis of steam generator tube creep rupture. During a hypothetical station blackout without auxiliary feedwater recovery, should the hot leg become voided, the pressurizer liquid will drain to the hot leg and flooding may occur in the surge line. The flooding model heavily influences the pressurizer emptying rate and the potential for surge line structural failure due to overheating and creep rupture.

The air-water test results in vertical tubes are presented in this paper along with a semi-empirical correlation for the onset of flooding. The unique aspects of the study include careful experimentation on large-diameter tubes and an integrated program in which air-water testing provides benchmark knowledge and visualization data from which to conduct steam-water testing.

1. Motivation for Improved Flooding Models for the Pressurizer Surge Line

Flooding is the situation in which the flow of a fluid in one direction is large enough to inhibit, partially or completely, the flow of a second fluid in the opposite direction and possibly cause a transition to unstable or cocurrent flow. Typically, a gas is flowing upward and a liquid is draining downward. The flow limitation is referred to as Countercurrent Flow Limitation (CCFL) and is experienced under a number of reactor conditions. Flooding can prevent sufficient coolant flow into the reactor core or other reactor components. The current project is to improve the level of understanding of flooding mechanisms and to develop an analysis model for more accurate evaluations of flooding in the PWR pressurizer surge line.

1.1 Occurrence of Flooding in Reactor Systems

There are several locations within the reactor cooling system where gravity drainage of liquid can be impeded by upward flowing vapor. These include the downcomer annulus, the upper core tie plate, the riser section of PWR inverted U-tubes and the pressurizer surge line. In the reactor vessel, flooding can occur during blowdown as Emergency Core Cooling liquid is attempting to fill the downcomer. During reflood, flooding can occur at the tie plate, where the upflow of steam prevents or limits the fallback of liquid (INEL, 1999; LANL and PSU, 2000). Flooding can disrupt condensation heat transfer in the riser section of a PWR U-tube during midloop operation and interrupt a mechanism of decay heat removal (Vierow, 2003). The pressurizer surge line is also a potential location for flooding during severe accidents and following a small break LOCA in some advanced light water reactors.

1.2 Need for Improved Flooding Models for the Pressurizer Surge Line

Interest in flooding has recently increased because CCFL in the AP600 pressurizer surge line can affect the vessel refill rate following a small break LOCA (Takeuchi, 1999) and because analysis of hypothetical severe accidents with the current simple flooding models show that these models represent the largest uncertainty in analysis of steam generator tube creep rupture (Vierow, 2004; Liao, 2005).

The safety systems of the AP600 are designed to depressurize the primary system following detection of a small break LOCA. The reactor coolant system pressure is depressurized down to the containment pressure to allow gravity feed of water from the in-containment refueling water storage tank (IRWST). The pressurizer may then be refilled because the top of the pressurizer is connected to the IRWST via depressurization valves. Integral tests were performed at the APEX facility (Takeuchi, 1999) to investigate system performance. Results showed that the pressurizer did not drain until after the final stage of depressurization valves opened. Flooding in the surge line is suspected to be the cause of the delayed drainage. The pressure drainage is important because the head in the downcomer due to draining pressurizer liquid influences the downcomer pressure, which in turn determines the IRWST coolant injection into the downcomer.

Recent severe accident analyses demonstrate the need to model flooding accurately in the pressurizer surge line, and highlight the primitive level of current modeling in severe accident analysis codes (Vierow, 2004, Liao, 2005, Burns, 2005). Some of these codes employ the same flooding models as in thermal hydraulic codes such as RELAP5. In analysis of hypothetical severe accidents and the TMI-2 accident by several codes, large uncertainties were shown to reside in the predictions of flooding in the pressurizer surge line. The flooding results greatly impact the calculated progression of the TMI-2 severe accident and the creep rupture behaviors of the surge line and steam generator tubes as described below.

There has been concern about steam generator tube creep rupture in hypothetical severe accidents, because it represents a bypass of the containment for radioactive materials to the environment. Best-estimate evaluation of the containment bypass release risk is critical to institute necessary measures to understand the risk. The Laboratory for Nuclear Heat Transfer Systems at Texas A&M University is identifying the analysis uncertainties involved in predicting the steam generator creep rupture and has

shown flooding in the pressurizer surge line to be one of the largest uncertainties (Vierow, 2004, Liao, 2005).

During a station blackout severe accident, coolant vents out of the primary system through the pressurizer power operated relief valves. When the accident progresses to natural circulation cooling of the core, the pressurizer is filled with water. The pressurizer pressure is about 160 bar, the liquid draining through the surge line is at its saturation temperature, and the gas flowing up the surge line is superheated, with an average of 25K above its saturated temperature. The draining of the pressurizer water to the hot leg affects the temperature rate of increase in the surge line pipe wall, which affects the surge line creep rupture behavior. The creep rupture failure timing of the surge line, on the other hand, may determine whether the surge line fails experiences structural failure before the steam generator tubes could fail. If the steam generator tube failure happens first, radioactive material may be released directly to the environment. Therefore, the flooding application in the surge line is important in realistic prediction of containment bypass release probability of radioactive materials.

In the TMI-2 severe accident, there were two locations where countercurrent flow was important. The first location was the pressurizer surge line. Here, the surge line was comprised of a number of pipe sections at various inclinations and flooding influenced the rate at which the pressurizer drained. The pressurizer drain rate via the surge line determined the rate at which the core could be cooled and the timing of heatup following the emptying of the pressurizer. The second location was the reactor vessel upper plenum, where liquid from the pressurizer flowed countercurrent to the steam generated by decay heat and fuel cladding-coolant reactions. Hence, flooding predictions greatly affect the progress of TMI-2 severe accident simulations.

Since no satisfactory mechanistic flooding models exist, current safety analysis codes employ empirical or semi-empirical correlations to evaluate the onset of flooding. By using their default flooding models, the SCDAP/RELAP5, MELCOR and MAAP severe accident codes produce significant discrepancies in surge line flooding predictions for a hypothetical station black severe accident (Vierow, 2004). The goals of this work are to obtain a better understanding of the phenomena and to develop models that will address the safety analysis needs for current and future reactor designs.

2. Goals of the Project

The primary technical goals of the current project are:

1. to investigate the effects of condensation and tube inclination on flooding for geometries and conditions applicable to the PWR pressurizer surge line
2. to advance the understanding of flooding mechanisms
3. to develop modeling methods for use in nuclear reactor safety codes

A unique aspect of this project is the careful conduct of complementary air-water and steam-water tests on large diameter (3-in. inner diameter) tubes. Secondly, the air-water tests provide visual data of the two-phase flow and experience in establishing annular flow and guidance in other operational procedures which would be difficult to develop with the steam-water test facility alone. Thirdly, the results will be applied to a representative PWR surge line geometry.

The significance of the research into flooding mechanisms lies in the contributions towards improved safety and reliability of current and future LWR's. The phenomena investigated in this work have the potential to occur in current and future reactors. The modeling methods that result from this study will provide a tool for evaluating system performance and will be necessary for the reactor design and licensing processes. The analysis models will be made compatible with a variety of reactor safety codes.

3. Previous Research on Flooding

Although a great deal of work has been carried out in the past few decades, there is still considerable uncertainty concerning the mechanisms causing flooding as well as the most appropriate correlations for practical applications. Several factors affect the onset of flooding, including the tube diameter, tube inlet and outlet configuration, tube inclination and fluid properties, to name a few.

Generally, there are two approaches to setting up a flooding model. One is an empirical or semi-empirical correlation that may contain constants from a numerical fit to experimental data. The formulation is generally expressed as a function of dimensionless variables that account for dominant phenomena and/or fluid properties. Another is a mechanistic model based on simplifying assumptions for the flooding physical mechanisms.

Due to the large number of influencing factors and the complexity of the mechanisms involved, a semi-empirical correlation is an efficient approach to predict the onset of flooding with some degree of physics modeling. However, the correlations that rely on constants from data fits are limited to the test condition ranges. On the other hand, no mechanistic models have shown satisfactory performance in predicting the onset of flooding for a variety of nuclear piping systems. A comparison of the performance of several empirical and semi-empirical correlations is presented by McQuillan (1985). Comprehensive surveys on flooding literature are presented by Bankoff (1983) and Hewitt (1996).

3.1 Experimental Investigations

Flooding is highly dependent on a number of experimental parameters including test section design, operating conditions and operating procedures. Care must be taken when comparing data from different programs to account for discrepancies in experimental programs. Some key studies and their findings are described below as they relate to the PWR pressurizer surge line situation. The justification for the design, operating conditions and operating procedures of the current air-water tests is provided in the following section.

Condensation effects

Condensation effects on flooding have been studied in vertical tubes and one study is known for tests at a nearly horizontal angle (Bankoff, 1983). Condensation effects were shown to cause a negative pressure loss due to loss of the vapor phase momentum. The Bankoff review also discussed the effect of liquid film temperature on steam condensation, as this influences the occurrence of flooding and the location of any flooding.

Several tests were conducted to investigate flooding in annular downcomer of a PWR, as summarized by Wallis (1980) and Rothe and Crowley (1978). A key finding from the Wallis steam-water study was that the steam-water data did not depend on the water temperature. The flooding process was therefore driven primarily by hydrodynamic phenomena, as opposed to heat transfer phenomena. In addition, Wallis' comparison of steam-water and air-water data showed reasonable consistency to nearly within the data uncertainty. However, scatter in the data led to the conclusion that secondary phenomena not included in empirical correlations were affecting flooding occurrence.

Visualization studies on flooding for a liquid/condensing gas mixture were reported by Girard et al., (1992). Girard observed steam/water flooding in a glass test section for imposed pressure drops across the tube at near atmospheric pressure.

Reflux condensation in a vertical tube with flooding has been studied by one of the authors to obtain local heat transfer coefficients (Vierow, 2003). In these experiments, steam was injected into the bottom of a stainless steel condenser tube and the conditions under which condensate did not return downward were recorded. Since flooding investigations were not the target of the study, critical information such as the conditions at onset of flooding was not pursued and flooding models were not developed.

Tube inclination effects

Flooding prediction in inclined tubes such as the pressurizer surge line is less conclusive than that in vertical tubes. Several studies on air-water systems have been conducted, primarily in channels with smaller diameters. Zapke (1996) and Mouza (2003) incorporated the effect of inclination angle into their correlations but the dependence of the flooding velocity on inclination angles has not been clearly pointed out.

To study the effects of inclination angle and upper end conditions on the onset of flooding (Wongwises, 1998), experiments showed that for an upper-open end system, with increasing inclination angles from the vertical, the flooding curves shift to lower gas velocities; for an upper-closed end system, the onset of flooding is nearly the same for all inclination angles. For steam-water countercurrent flow in an inclined channel (Lee, 1983), the flooding steam velocity was the lowest for the smaller inclination angles and increased with an increase in inclination up to approximately 30°; for 31° and 87°, the flooding steam velocities were approximately equal. In a study (Barnea, 1986) for air–water countercurrent flow in a 51 mm tube for a wide range of inclination angles (1° – 90° from horizontal), it was pointed out that the critical flooding velocity tends to increase and then decrease as the inclination angle is changed from horizontal to vertical.

Comparing the limiting velocity in vertical tubes and inclined tubes (Takeuchi, 1999), the counter-current flow in the vertical section limits the liquid downflow more than the inclined section; flooding becomes less limiting with increasing inclination below 45°, and becomes more limiting with increasing inclination above 45°. In a nearly horizontal pipe with inclination angle less that 1° (Choi, 1995), the transition criterion for the onset of flooding is very sensitive to the inclination angle; a slight increase in the inclination angle has a great effect on the location where flooding occurs and on the flow patterns.

Wu and Vierow (2006) conducted condensation experiments for cocurrent steam/water flow in horizontal tubes. Detailed temperature measurements demonstrated that condensation in horizontal and inclined tubes is very different from that in vertical tubes, often with higher heat transfer rates due to better contact of the steam with the cooling surface on the upper tube portion. The amount of condensation heat transfer to cooler liquid film and tube wall surfaces will determine whether the steam flow rate is sufficient to induce flooding, and if so, at what location.

3.2 Development of Empirical Correlations

Air-water correlations for vertical tubes

Under the simple geometry of a vertical tube and normal temperature and pressure conditions, the Wallis correlation and the correlation using the Kutateladze parameter are the most well established empirical formulations for flooding prediction. The Wallis correlation considers the tube diameter D, and fluid densities ρ_f and ρ_g, while the correlation with the Kutateladze parameter, Ku, considers the fluid densities ρ_f and ρ_g, and surface tension σ.

Wallis correlation:
$$\sqrt{j_g^*} + m\sqrt{j_f^*} = c \tag{1}$$

where
$$j_f^* = \frac{j_f}{\sqrt{gD(\rho_f - \rho_g)/\rho_f}} \text{ and } j_g^* = \frac{j_g}{\sqrt{gD(\rho_f - \rho_g)/\rho_g}} \tag{2}$$

Kutateladze-type correlation:
$$\sqrt{Ku_g^*} + m\sqrt{Ku_f^*} = c \tag{3}$$

where
$$Ku_g = \frac{j_g}{\sqrt[4]{g\sigma(\rho_f - \rho_g)/\rho_g^2}} \text{ and } Ku_f = \frac{j_f}{\sqrt[4]{g\sigma(\rho_f - \rho_g)/\rho_f^2}} \tag{4}$$

In equation (1), j_g and j_f are the volumetric fluxes of the gas and liquid phases, respectively. The coefficients m and c depend on tube geometry and inlet/outlet configuration and are correlated from experiment data (Wallis, 1969). It has been suggested that m and c can be obtained as variables explicitly dependent on tube geometry and inlet/outlet configuration (Jeong, 1996; Vijayan, 2001).

Chung et al. (1980) presented a well-known modification of the Kutateladze-type correlation, however Zapke and Kroger (2000) showed that this formulation does not reproduce flooding data for 30 mm (smaller diameter tubes) well.

$$\sqrt{Ku_g^*} + m\sqrt{Ku_l^*} = c_1 \tanh\left[c_2\left(Bo^{1/8}\right)\right] \tag{5}$$

where Ku is defined following equation (3), the Bond number, Bo, is as:

$$Bo = \frac{\left(\rho_l - \rho_g\right) gD^2}{\sigma} \tag{6}$$

and $c_1$and c_2 are empirical constants.

The dimensionless parameters defined by Wallis and Kutateladze are related by the Bond number. The Kutateladze number, Ku, is a ratio of inertial forces to buoyancy and surface tension forces. This is an appropriate parameter when the liquid film is thin and the gas flow perturbation around the film is independent of the tube diameter. Wallis and Makkenchery (1974) explain that in very small tubes, the surface tension effect may be strong enough to cause bridging of the liquid film across the tube. Even for a zero gas velocity, liquid holdup may be possible. The force balance of buoyancy to surface tension is the Bond number shown in the Chung correlation (Eq. (5)). The Wallis gas velocity for flooding, j_g^*, may then be related to the Kutateladze number as:

$$j_g^* = \frac{Ku}{Bo^{1/4}} \tag{7}$$

Consistent with this analysis, the Kutateladze parameter and the Wallis gas velocity for flooding have been found to be more appropriate for large diameter and small diameter tubes respectively (Jayanti, 1996). Although it is expected that the Kutateladze-type correlation may be applicable to the surge line situation, comparison against the experimental data from the current program will be shown to contain unacceptably large discrepancies.

Zapke and Kroger (2000) present a recent evaluation of dimensionless parameters for correlating flooding data. Through a discussion of properties and flow conditions that could affect flooding, they show that the Froude number and the Ohnesorge number best reproduce flooding data. The Froude number is a ratio of inertial to buoyancy forces while the Ohnesorge number is a ratio of liquid viscous to surface tension properties.

Froude number: $$Fr = \frac{\rho_f V_f^{\,2}}{gD_h\left(\rho_f - \rho_g\right)} \tag{8}$$

Ohnesorge number: $$Oh_f = \sqrt{\frac{\mu_f^{\,2}}{\rho_f D_h \sigma}} \tag{9}$$

The gas Froude number was found to be a function of the liquid Froude number to the 0.2 power multiplied by the liquid Ohnesorge number to the 0.3 power. While the coefficients change, these parameters will be shown to best reflect the data presented herein for flooding in large diameter tubes.

Steam-water correlations for vertical tubes

Several tests were conducted to investigate flooding in annular downcomer of a PWR, as summarized by Wallis (1980) and Rothe and Crowley (1978). These studies indicate that results may be presented as a dimensionless volumetric steam flux for flooding (j_g^*) obtained from the conventional dimensionless volumetric steam flux corrected by a factor involving the Jacob number to account for a steam flow reduction due to condensation.

Air-water correlations for inclined tubes

The correlations described previously do not account for the effects of condensation or tube inclination. The correlations that describe tube inclination effects are similar in format to the Wallis correlation but they include an additional factor that depends on tube inclination (Zapke, 1996).

Liao and Vierow (2006) surveyed experimental data for inclined tubes and proposed a simplified analytical model to predict the optimal channel inclination for maximum gas venting. The model assumes that flow regime transition occurs by Kelvin-Helmholtz instability and adopts a previously published criterion for onset of flooding in inclined channels. The liquid flow is restricted to laminar flow and the liquid film thickness must be much less than the channel height. The existence of the optimum channel inclination is the combined effects of conflicting mechanisms that govern the onset of flooding inside inclined channels. As the channel inclination varies from horizontal to vertical, the liquid film thickness becomes smaller. Consequently, the interfacial shear stress also decreases since the roughness of the interface decreases with a smaller film thickness. These effects result in increasing gas superficial velocity at the onset of flooding. The gas superficial velocity also increases due to the increasing gravity component tangent to the interface which has to be overcome in the direction of the gas flow. On the other hand, the gravity component normal to the interface diminishes, therefore the interfacial waves tend to be more unstable and the tendency for the onset of flooding is enhanced as the channel inclination varies from horizontal to vertical. Consequently, the gas flooding velocity tends to decrease. The relative importance of these mechanisms determines the optimum channel inclination.

Correlations for PWR surge line situation

The Wallis and Kutateladze-type correlations were correlated from experiment data on air-water countercurrent flow in vertical tubes under normal temperature and pressure conditions. Prediction of flooding in the pressurizer surge line is difficult due to the complex geometry of the surge line. Another difficulty in applying flooding models for safety analysis arises from high temperature and pressure conditions during severe accidents, where the fluid properties and interfacial reactions are drastically different from normal condition.

From the above literature review, it was observed that no flooding model is generally applicable to a variety of conditions, especially in the pressurizer surge line with inclined tube sections and condensation heat transfer.

3.3 Development of Mechanistic Models

For a discussion of mechanistic models, the reader is referred to the companion paper presented at this workshop (Hogan, 2008).

4. Scaling of Experimental Facility

4.1 Geometry

Tube diameter is a primary factor that must be properly scaled in the experiment. Tube diameters are commonly divided into two broad groups, large diameter and small diameter. Since a reference PWR pressurizer surge line diameter is 10 in., the experimental facility must have a large-diameter test section.

The surge line geometry is particular to each reactor and may consist of several pipe sections at various inclinations. For the current project, focus is placed on the pipe section connected to the pressurizer. Descriptions of the diffuser at the bottom of the pressurizer tank, which determines the water flow configuration into the surge line, are generally not available.

Two types of diffuser configurations are described herein (Fletcher, 2005). In one configuration, the cylindrical wall of the surge line is extended about 2 feet into the bottom of the pressurizer tank and is capped on top with a solid circular plate. Flow passes through rectangular axial slots located around the periphery of the cylindrical pipe. In the second configuration, the surge line is terminated with a smooth penetration on the bottom of the tank and the diffuser is a hemispherical screen covering the surge line opening on the bottom of the tank. The screen is constructed of perforated plate with circular holes. The current investigations make the simplifying assumption that the diffuser configuration will produce a liquid film around the inner periphery of the surge line, for annular flow.

4.2 Initial and Boundary Conditions

As predicted by the SCDAP/RELAP5 code, for a typical 4-loop Westinghouse PWR in natural circulation during a hypothetical station blackout (Vierow, 2004), the flow regime in the junction where the surge line connects to hot leg is bubbly flow, while the flow regime in the junction where the surge line connects to the pressurizer is either slug or annular flow. The gas upflow velocity is in the range of 1 m/s to 7 m/s. Liquid downflow occurs at the lowest gas flow rate when the PORV is closed. The pressurizer pressure is about 160 bar, the liquid draining down in the surge line is at its saturation temperature, and the gas flowing up in the surge line is superheated, with an average of 25K above its saturated temperature.

4.3 Results of Scaling Analysis

In designing the test facility and determining test conditions, the important parameters for flooding phenomena in Table 1 were identified.

Table 1

Parameter	Effect/Importance	Reference
Tube diameter	Relative importance of capillary, inertial and buoyancy effects, other/High importance	Vijayan (2001), Jayanti (1996)
Tube length	Flooding location	Jeong (1996)
Surface tension	Stabilizing effect on flooding/Medium importance	Deendarlianto (2004)
Fluid density ratio	Disturbance and instability effects/High importance	Zapke (1996)
Liquid Re	Film thickness, stability/High importance	Carvalho (1998)
Gas Re	Minimal effect on flooding/Low importance	Zapke (1996)
Liquid viscosity	Interfacial instability/Differing conclusions on importance	Chung (1980), Zapke (1996)
Gas Viscosity	Minimal effect on flooding/Low importance	Zapke (1996)

Based on experimental data for several tube sizes, Vijayan (2001) proposes that tube diameters exceeding 67 mm be considered large. An inner diameter of 3 inches (76.2 mm) was selected for the current experiments. A tube length of 72 inches was chosen to allow sufficient length for flooding and for possible variation in the flooding location between air/water and steam/water tests.

The fluid density ratio under PWR cannot be reproduced in the air-water tests. The steam-water tests will have a lower steam-to-water density ratio than in the actual system because the tests will be run at lower pressure. Rothe and Crowley (1978) addressed pressure scaling issues and concluded that for saturated water behavior in small-scale facilities, the dimensionless Wallis j^* parameters properly scale the effect of system pressure. This argument will be addressed in future steam-water testing.

Liao (2005) evaluated the expected conditions and estimated a liquid Re of about 218,000, based on j_f of 0.1 m/s, a system pressure of 160 bar and temperature of 630K. This Re cannot be preserved in the laboratory experiment; however, the liquid Froude number can be. The liquid-phase Froude number is estimated at 4×10^{-4} for the actual system. The same liquid Froude number requires a $j_{f\,of}$ 0.055 m/s in the current air-water test facility. The corresponding water volumetric flow rate of 4.2 GPM is within the capabilities of the present facility.

Chung (1980) reasoned that an increase in liquid viscosity will result in flooding at a lower air flow rate because waves on the film surface are formed with smaller radii of curvature. Counteracting this destabilizing effect, viscosity also has a damping effect on interface oscillation, thereby delaying the onset of an instability. The destabilizing effect of increased liquid viscosity was confirmed by experiment; however, the effect is only important when the viscosity is changed by an order of magnitude or more. Zapke and Kroger (1996) refute the conclusion that liquid viscosity has a small effect, by plotting Chung's data in terms of dimensionless parameter that demonstrates the non-negligible effect of liquid viscosity.

The results of the scaling analysis are provided in Table 2. From scaling calculations, the test facility pressure is maintained between 1 and 4 bar. Pressure and temperature scaling will be considered in the steam/water tests. Major goals of the air/water tests are to provide a basis for the design of the steam/water test facility and to permit visualization data. Thus, some features of the steam/water behavior are not reproduced in the air/water tests.

Table 2 Scaling of Surge Line Specifications and Reactor Conditions

Parameter	Actual Surge Line	Experiment	Comment
Tube diameter, D (inches)	10	3.0	Classified as "large diameter"
Tube length	Reactor-specific	72 inches	
Tube inclination (degrees)	0 - 90	0 - 90	Actual surge line is comprised of multiple pipe sections.
Pressure (bar)	160	1 – 4	Determines fluid density ratio. To be addressed in steam/water tests,
Air temperature	Saturated steam to 25 K superheat	Room temperature	to be addressed in steam/water tests
Water temperature	Subcooled to saturated	Room temperature	to be addressed in steam/water tests
Liquid Froude number	4×10^{-4}	4×10^{-4}	j_f of 0.055 m/s in experiment, water flow rate of 4.2 GPM is within capabilities

5. Air/water Testing

5.1 Experimental Facility

A schematic of the experimental system is shown in Figure 1. A blower supplies air to the bottom of the test section and an annular film is created at the top. The facility is capable of having the test section inclined at angles between horizontal and vertical to capture phenomena in the various possible surge line inclinations. The test tube is a 72-inch long, 3-inch inner diameter acrylic tube with the water inlet/air outlet at the top and the water outlet/air inlet at the bottom. All acrylic components are optically transparent.

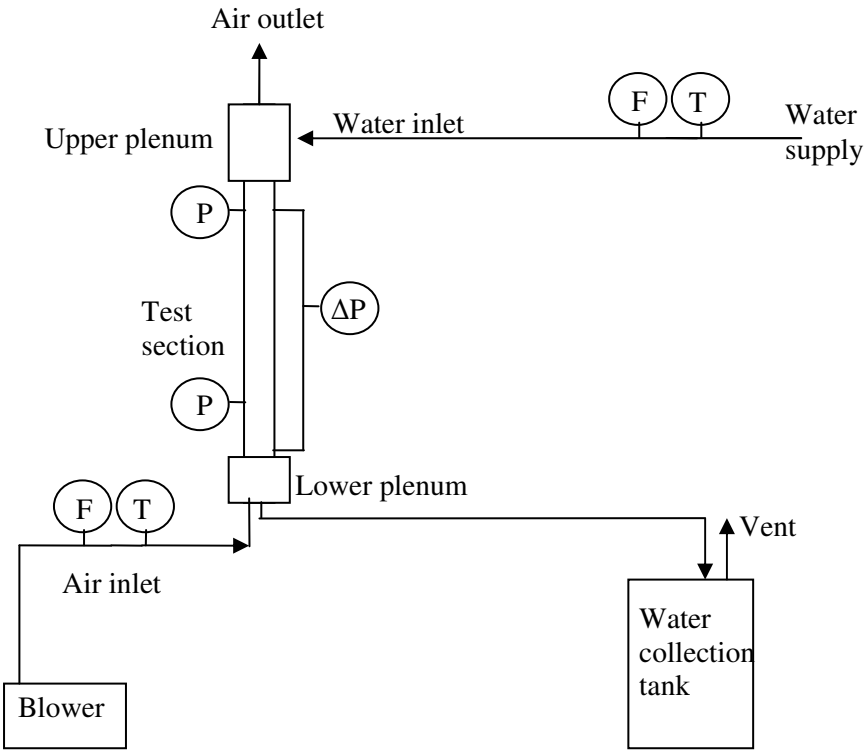

Figure 1 Air/water Test Facility Schematic

Particular care was given to the design of the water inlet to enable a smooth liquid film falling along the inner surface of the test tube. The water injection plenum was designed for creating an annular falling film in the test section while allowing for the unimpeded flow of air out of the system. During flooding, water also exits the top of the test section through this path. The design, shown in Figure 2, consists of a 6-inch long, 5-inch ID upper plenum encompassing the 3-inch ID, 0.25-inch thick test section tube. Two 1-inch NPT threaded inlet holes facilitate symmetric water injection into the plenum. To achieve annular flow within the test section, a 6-inch long, 2.75-inch OD acrylic tube section is inserted to create a 0.125-inch thick annular region inside the test section tube. Twelve 0.25-inch diameter holes were drilled through the test section tube, 1 inch above the bottom of the insert, spaced equally around the test section tube. Water flows through these twelve holes, forming a liquid film around the inner surface of the test section tube. This insert also provides a means by which air and water droplets can be removed from the test section with a minimal pressure drop.

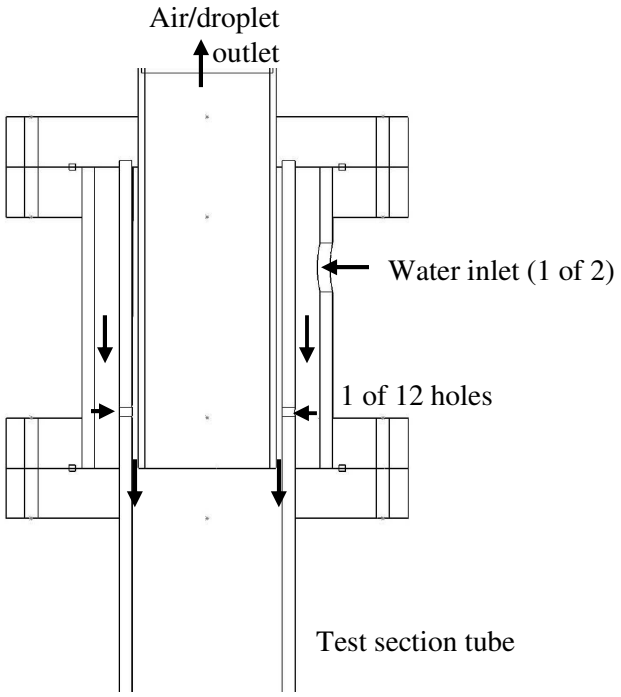

Figure 2 Upper Plenum with Water Flow Paths Shown for Annular Film Formation

The lower plenum is identical to the upper plenum, except for absence of the water injection ports. The lower plenum serves as a transfer tank for the water leaving the bottom of the test section. During the tests, it also serves as a viewing chamber for water leaving the test section and the exhaust section of the air inlet.

A blower is used to inject air into the air inlet section in the lower plenum. A blower from the Republic Company, model HRB201, was acquired. The maximum air flow rate is 102 cfm at 42 in. of water maximum pressure drop. An entrance length of 30 L/D in straight pipe delivers the air with a fully developed velocity profile. Since the air is highly turbulent, it is assumed that the profile is uniform over the cross section entering the test section tube, although characterization tests will be done as future work.

5.2 Instrumentation

A National Instruments data acquisition system records the data and displays various parameters via a LabView program. Except for the rotameters on the water lines, all data is sent to the data acquisition system and electronically stored. Data sampling is done at a 10 Hz rate, although much higher rates are possible with this system.

The water inlet flow rate is measured with a ½-in. Yamatake MGG-18D magnetic flow meter located upstream of the test section. For water flow control, two Dwyer flow meters are installed between the magnetic flow meter and the test section.

A Pitot tube with a static pressure port is installed at 30 L/D downstream of the blower to measure the stagnation and dynamic pressures of the fully developed air in the approach pipe. The dynamic pressure is therefore known, which in turn provides the air centerline velocity. From the fully developed velocity profile for turbulent flow, the average air velocity across the test section is calculated. With the accompanying temperature measurement, the air density can be determined, and finally the air mass flow rate is known.

The air inlet temperature and water inlet temperatures are measured with Type T thermocouples.

A Honeywell model STD924 differential pressure transducer measures the pressure drop along the test section. The pressure ports are 52 inches apart and are located above and below the expected

flooding locations. A change in the pressure drop along the test section is known to accompany the occurrence of flooding and this data aids in precisely identifying the instant of flooding onset. Honeywell model STA940 absolute pressure transducers measure the pressure at elevations close to those of the differential measurement.

The images are recorded by a CMOS camera (IDT X-Stream XS-4) with a resolution 512 (H) x 512 (V) pixels of a size of 16 × 16 μm^2. The camera was fitted with a 55 mm (f /2.8) Nikon lens. The resulting image area covered by the camera for these set of experiments is 1.5*d* (H) × 1.5*d* (V) or approximately 80 mm × 80 mm. Here, *d* is the inner diameter of the test section. The images were acquired at the rate of 3000 frames per second with an exposure time of 330 μs.

5.3 Experimental Procedures

The procedures for running this experiment require that annular flow for a given water flow rate be established and the air flow rate increased incrementally until flooding is observed. A test commences with an air flow rate that is too low to induce flooding. The air flow rate is increased by changing the position of a blower bypass valve and letting the system establish a new steady state for at least 5 minutes. If flooding does not occur within a 5 to 10 minute period, the air flow rate is increased again.

Both sustained flooding and flooding followed by a return to a steady state were observed. The air flow rate for sustained flooding was taken to determine the requirements for flooding conditions.

The state of annular flow can be observed in the test section and in the lower plenum. The bottom of the test section is clearly visible through the lower plenum. Furthermore, it is also possible to look down the air outlet pipe as another form of visual inspection.

The tests reported herein are for the vertical tube. Future air/water tests will include data for tube inclination from the vertical.

5.4 Test Matrix

From the previous discussion of expected conditions in a reactor, the water volumetric flow rate of 4.2 GPM must be within the test matrix. The region of interest corresponding to reactor conditions and the test matrix that is possible within the lab are shown in Table 3. The upper and lower limits are determined by the capabilities of the experimental facilities.

Table 3 Test Matrix

Fluid	Water [GPM]	Air [m/s]
Upper limit	7.1	40.0
	6.7 6.3 5.9 5.5 5.1	
Region of Interest	4.7 4.3	
Lower limit	3.9	32.4

5.5 Experimental Results

Characterization tests were run to confirm various aspects of the facility. Details may be found in Solmos (2008). The only characterization test reported herein is for confirmation of annular flow. The water inlet design successfully produced a thin water film around the complete inner surface of the test section tube. The film was visible through the acrylic tube and through the acrylic lower plenum as water drained from the test section into the lower plenum. Photographs were taken of the film looking down the air outlet tube, which further confirmed the existence of a thin film along the complete circumference and along the entire tube length.

For a given liquid flow rate, the air flow rate was increased incrementally, allowing at least 5 minutes for flooding to occur. Once flooding was observed, the air flow rate was recorded and then reduced to a rate at which flooding was not sustained. This provided one data point for flooding. Subsequent runs were conducted by repeating this process, with smaller incremental increases of the air flow rate as the flooding point was approached. An example of a run is shown in Figure 3. The pressure gradient along the test section is plotted as a function of air velocity, as the pressure gradient was a sensitive indicator of flooding.

Figure 4 shows the quasi-steady nature of the system prior to flooding for an air velocity that led to flow reversal. The air velocity oscillated about a constant value for about 700 sec. before flooding was observed. Upon flooding, the velocity dropped significantly and exhibited a highly turbulent behavior. Because the air supply (blower) reacted to flooding, only the data up to the onset of flooding reflects the phenomena postulated to occur in the reactor situation.

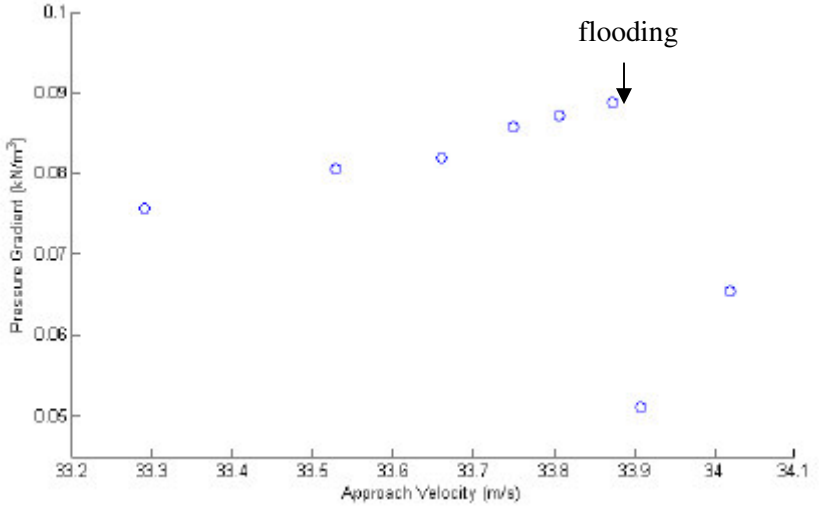

Figure 3 Approach to Flooding by Incremental Increase of Air Velocity

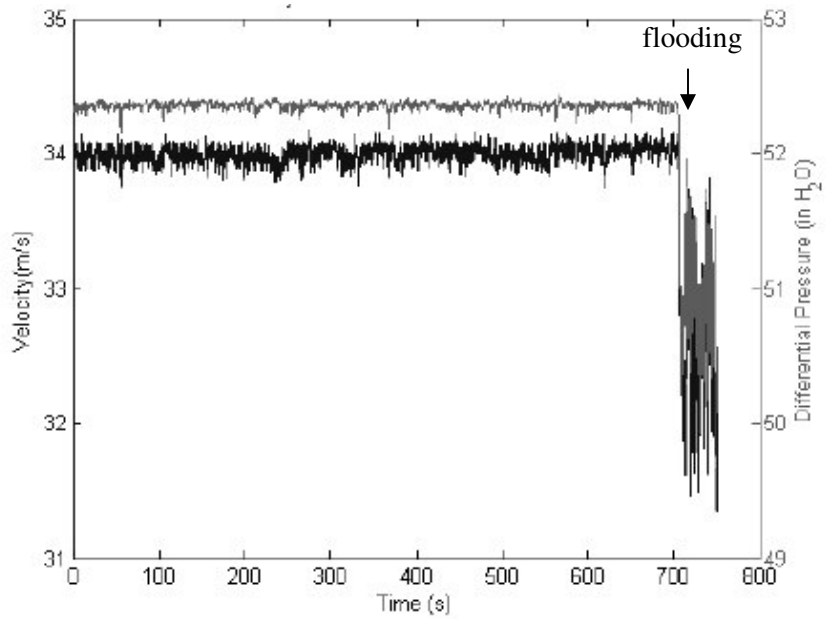

Figure 4 Change in Flow Conditions Due to Flooding

Flooding resulted in the formation of a visible wave towards the bottom of the test section, always above the bottom pressure port. That is, it was not caused at the test section bottom entrance. This wave proceeded up the length of the test section carrying a portion of the test section water. A sequence of the flooding evolution is shown in Figure 5. This series of pictures was taken at a frame rate of 2000 Hz.

While the sequence is more meaningful when observed as a video, the flow complexity is illustrated. Droplets can be seen, along with wave formation along the inner periphery of the tube.

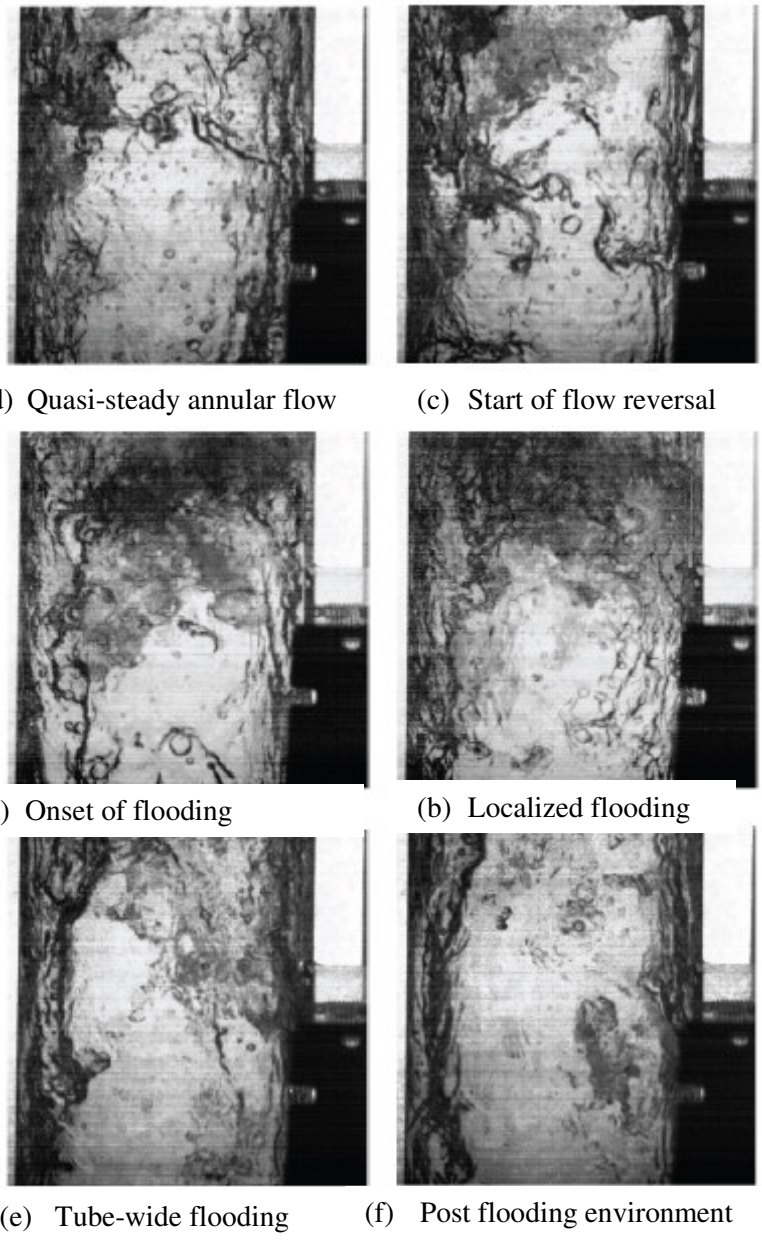

(d) Quasi-steady annular flow (c) Start of flow reversal

(a) Onset of flooding (b) Localized flooding

(e) Tube-wide flooding (f) Post flooding environment

Figure 5 Flooding Visualization

The data have been classified according to flooding behavior. For a given liquid flow rate, relatively low air flow rates did not induce flooding. Over a range of higher flow rates, unsustained flooding was observed. That is, flooding would be observed and then the system would return to a quasi-steady state.

There was no regular time constant for the flooding in this "unstable flooding band" of air flow rates and flooding occurred only once for some flow rates. The lowest flow rate at which flooding was sustained is considered the flooding velocity. Due to this flooding band, care was taken to give the system ample time to establish a steady state. Each air velocity was run for at least 10 minutes to determine the flooding behavior, unless it was clearly a sustained flooding case.

The minimum air flow rate that caused sustained flooding for each liquid flow rate was selected for development of an analytical model. The data are presented in terms of dimensionless volumetric fluxes, j_g^* and j_f^*, as defined in Equation (2), to be consistent with current convention. These data with error bars are shown in Figure 6.

The error in each data point was quantified based on random error and systematic errors. To evaluate the random error, each test was repeated at least once. Further, the random error was statistically evaluated by repeating the 6.8 GPM liquid flow rate test 20 times. The standard deviation in the flooding velocity was found to be 0.16 m/s, or 0.5% due to randomness.

For the systematic error, uncertainties due to instrumentation error, geometric measurements, unit conversions and equipment calibration were propagated using standard error propagation techniques. The total error is reported as error bars in the final data presentation.

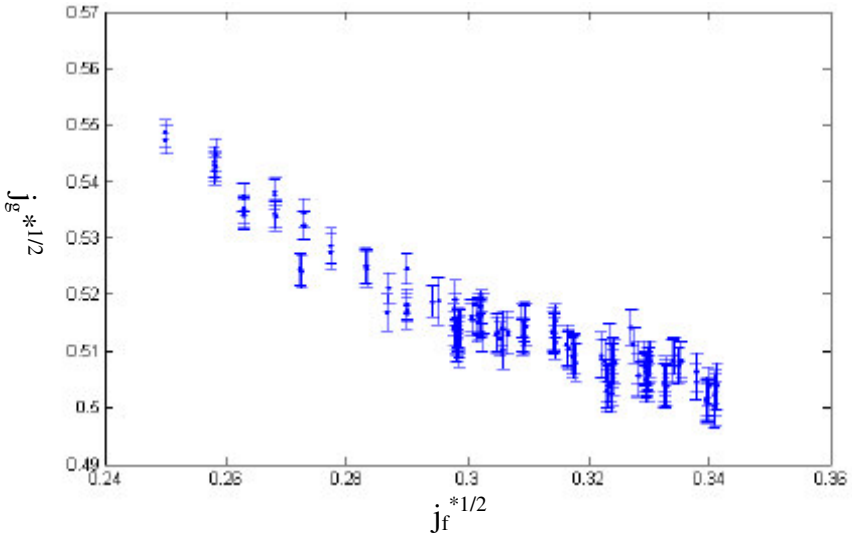

Figure 6 Experimental Data with Error Bars

6. Analytical Model Development

6.1 Application of Current Flooding Models in Reactor Safety Codes

Current major US design basis accident safety analysis codes, RELAP5 and TRAC utilize Wallis or Kutateladze-type correlation, or a hybrid between these two flooding correlations to predict limiting flow rates in the countercurrent flow (INEL, 1999; LANL and PSU, 2000). In order to utilize these correlations for safety analysis, empirical correlation coefficients are estimated from correlated data by experiments on prototypical or scaled down test facilities. Similarly, US severe accident codes such as SCDAP/RELAP5 have adopted flooding models based on Wallis-type correlations. In MELCOR, the flooding curve is used to generate co-current interfacial friction parameters (Gauntt, 2005), as opposed to a direct estimation of flooding occurrence.

These correlations were tested against the data acquired herein, as shown in Figures 7 and 8 respectively. Given that the Wallis correlation is applicable to smaller tube diameters, the discrepancy between test data and predictions is not surprising. Both the slope and the magnitudes show large error.

The Kutateladze-type correlation provides a better prediction of the slope and magnitude, although improved predictive capabilities are desirable.

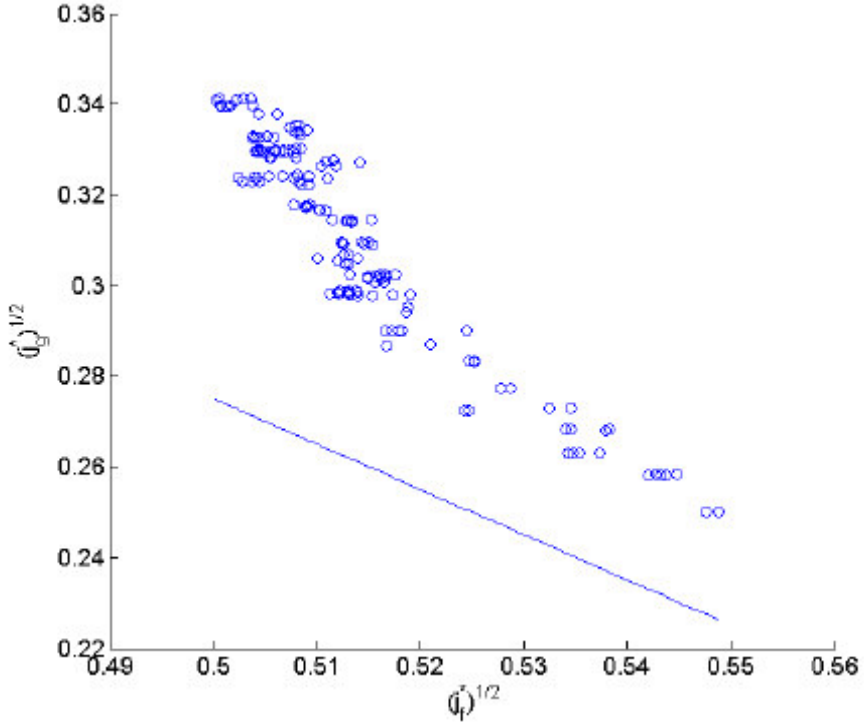

Figure 7 Wallis Correlation Prediction of Current Experimental Data

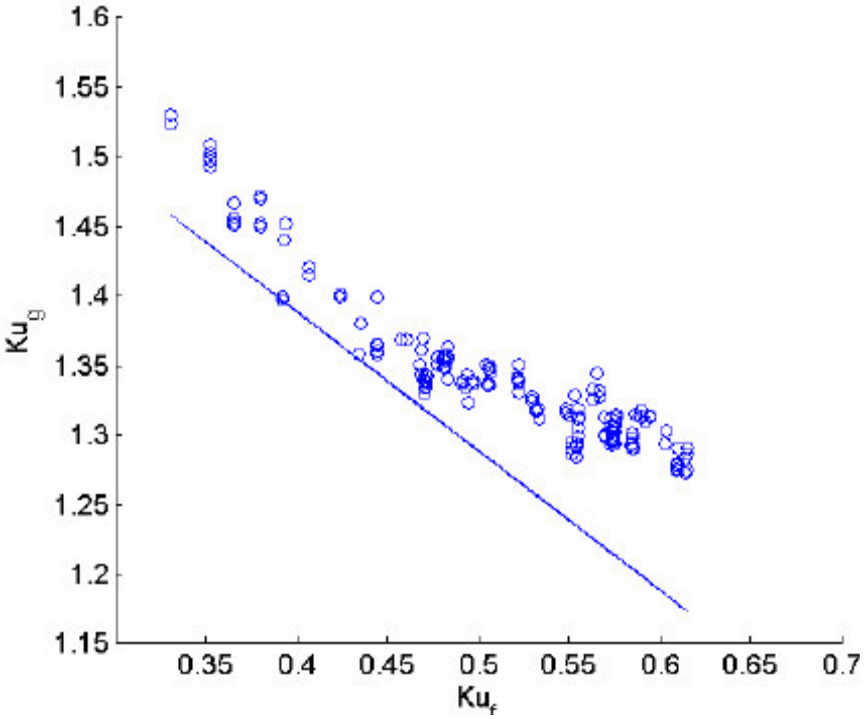

Figure 8 Kutateladze-type Correlation Prediction of Current Experimental Data

6.2 Empirical Model Development

As discussed with regard to correlation development, the physics and the fluid properties may be represented by the Froude number and the Ohnesorge number.

The Froude number is the ratio of inertial to buoyancy forces. To correlate flooding data, the Froude number has been calculated based on the relative velocity of the fluids. Since the tube is considered a large-diameter tube, radial effects are expected to be minimal and a more appropriate characteristic length is the film thickness. A modified Froude number is defined as below.

$$Fr_m = Fr\left(\frac{\delta}{D}\right)^{-2} \tag{10}$$

The film thickness is obtained from a formulation by Belkin et al. (1959) for annular flow along vertical walls:

$$\delta = 0.135\frac{\nu_f^{2/3}}{\left[g\left(1-\frac{\rho_g}{\rho_f}\right)\right]^{1/3}}\mathrm{Re}_f^{7/12} \tag{11}$$

where the liquid Reynolds number is defined as:

$$\mathrm{Re}_f = \frac{j_f D}{\nu_f} \tag{12}$$

and the superficial liquid velocity is the ratio of liquid volumetric flow rate over flow area.

The Ohnesorge number is a ratio of liquid viscous to surface tension properties. Here too, the liquid film thickness is a more appropriate characteristic length than the tube diameter. The Ohnesorge number has been calculated as:

$$Oh_f = \sqrt{\frac{\mu_f^{\,2}}{\rho_f \delta\sigma}} \tag{13}$$

The data obtained in this investigation has been correlated in the following form:

$$Fr_m^{0.1} - 0.1m\,Oh_f = C_{\exp} \tag{14}$$

where the constants m and C_{exp} are $1.17\text{x}10^3$ and 1.93 respectively.

$$Fr_m^{\,0.1} - 1.17\times10^3\,Oh_f = 1.93 \tag{15}$$

Figure 9 shows the linearity of the data due to the exponent on the modified Froude number. The error bars show the error of about 3%. The error bands represent +/- 5% uncertainty.

The new correlation was validated against the experimental data of Lacy and Dukler (1994). These data were obtained for an aqueous NaCl solution (0.12 wt%) which was released through a porous tube section into a 50.8 mm inner diameter acrylic tube in annular flow. Air was injected at the bottom of the acrylic tube. This study concluded that wave growth and bridging across larger diameter tubes is not the

initiating mechanism for flooding. In the Lacey experiment, a change of direction of the liquid film velocity distribution in the region of the porous-tube water feed zone was studied by film thickness and pressure gradient measurements. The mechanism for this change of direction was suggested as the cause of flooding.

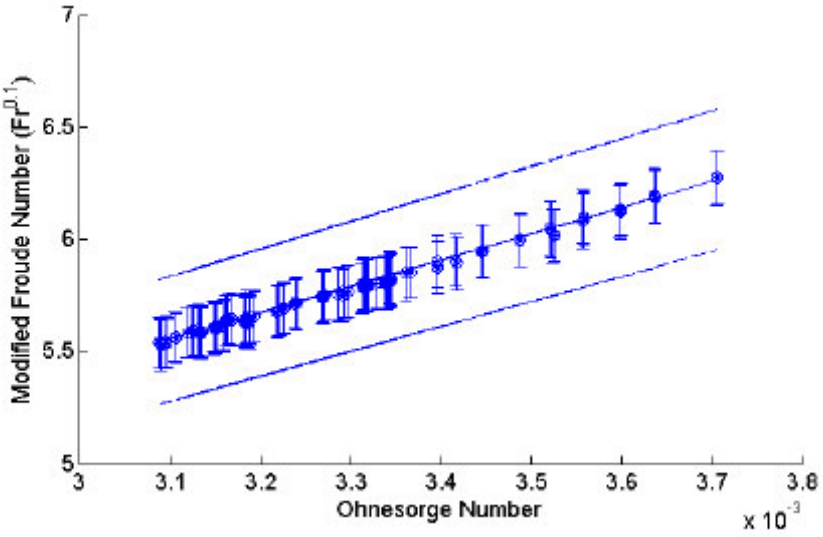

Figure 9 Modified Froude Number vs. Onhesorge Number for Current Experimental Data

Since this data had similar conditions as the present experiment, calculations by the proposed correlation were compared against the Lacy data. Figure 10 reveals in a plot of modified Froude number vs. Ohnesorge number that the trend is reproduced well. The average difference between data and analysis is 7.9% overprediction. At low Ohnesorge numbers, the error is about 6%, increasing to about 11% at the upper end of the range. Possible sources for the discrepancies are the water injection method and the tube diameter. Lacy's tube diameter of 50.8 mm is below Vijayan's proposed large-diameter criteria of 67 mm.

While the correlation provides reasonable results, the authors are pursuing data collection over a wider range of liquid and air flow rates to cover a wider range of operating conditions.

7. Conclusions and Future Work

An experimental and analytical program is being conducted to develop predictive models for flooding in the surge line of a PWR. To this end, an air-water flooding experiment has been carried out in a 76 mm inner diameter, vertical acrylic tube. The data provided a semi-empirical correlation for flooding in terms of a modified Froude number and the Ohnesorge number. Future testing will include a wider range of boundary conditions and tube inclination.

The visualization data has demonstrated the location of flooding and has enabled correspondence of the timing of velocity and pressure changes with the timing of flooding. Further assurance of the data quality was also provided via confirmation of annular flow in the test section, symmetry and other characterization tests. Efforts are currently being made to obtain images of the film and waves, to reveal the film thickness, wave frequency and growth and other parameters that influence the onset of flooding.

The knowledge obtained from the air-water testing is providing a basis for the steam-water facility design and testing procedures. In particular, procedures for establishing a liquid film around the inner circumference of the test tube and for test operation to obtain a quasi-steady state prior to flooding were developed. Air-water data will be acquired in the stainless steel steam-water facility to benchmark against the air-water data from the acrylic test facility. The two facilities have been designed to be as

similar as possible. Discrepancies in the air-water data are expected due to differences in water flow along a stainless steel surface and an acrylic surface and unavoidable design changes; however, these discrepancies are expected to appear as quantitative shift in the data on a dimensionless parameter plot, rather than a change in phenomena.

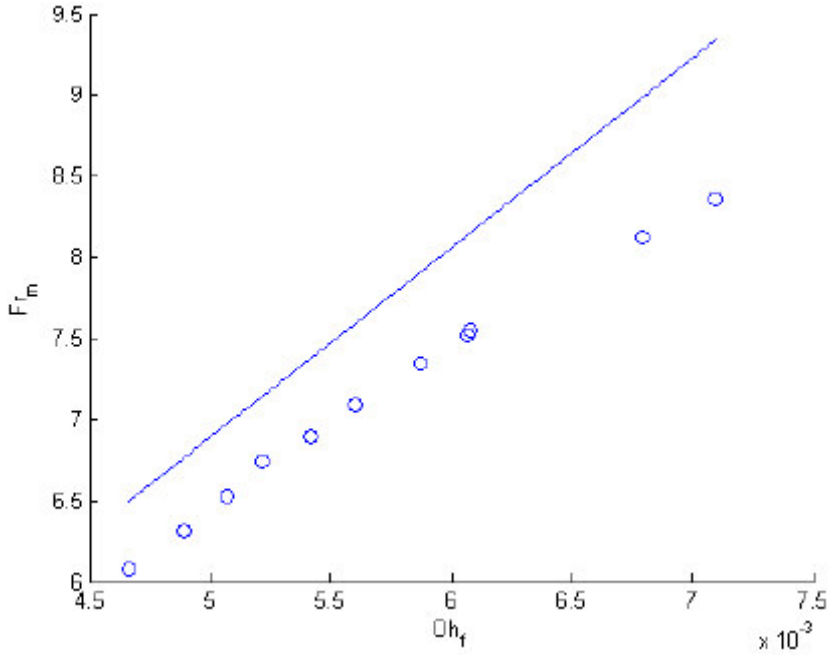

Figure 10 Comparison of New Correlation against Lacy (1994) Data

Empirical correlations for convenient implementation into reactor safety codes and mechanistic models for improved understanding of the phenomena are being developed. Hogan et al. (2008) discusses the effort towards the mechanistic modeling.

While these experimental programs are providing valuable data for well-defined geometries, they do not completely represent the situation in the surge line of a PWR. Prediction of flooding in the pressurizer surge line is difficult due to the complex geometry of the surge line and the various possible configurations for water entrance into the surge line. Another difficulty in application of flooding models for reactor safety codes arises from the high temperature and pressure condition during severe accidents, where the fluid properties and two-phase interactions are different from those at experimental conditions. These factors will be considered in the model development and uncertainties will be noted. Rothe and Crowley (1978) addressed pressure scaling issues and concluded that for saturated water behavior in small-scale facilities, the dimensionless Wallis j^* parameters properly scale the effect of system pressure. This point will be addressed in future steam-water testing.

Acknowledgments

The authors gratefully acknowledge financial support of this project by the US Department of Energy Nuclear Engineering Education Research (NEER) Project, Award No. DE-FG07-05ID14696.

References

Bankoff, S.G. and Lee, S.C. (1983). A critical review of the flooding literature. NUREG/CR-3060, Dept. Chem. Eng., Northwestern U., Evanston, IL.

Barnea, D., Ben Yosef, N. and Taitel, Y. (1986). Flooding in inclined pipes—effect of entrance section. *Can. J. Chem. Eng*., Vol. 64, p177–184.

Belkin, H. H., MacLeod, A.A., Monrad, C.C., and Rothfus, R.R. (1959). Turbulent liquid flow down vertical walls. *AIChE Journal*, Vol. 5, p245-248.

Burns, C., Liao, Y., Vierow, K. (2005). MELCOR Code Assessment by Simulation of TMI-2, Proc. of 11th International Topical Meeting on Nuclear Reactor Thermal Hydraulics (NURETH-11), Avignon, France, (18 pp.)

Guedes de Carvalho, J.R.F., and Talaia, M.A.R. (1998). Interfacial shear stress as a criterion for flooding in counter current film flow along vertical surfaces. *Chem. Eng. Sci*., Vol. 53 p2041-2051.

Choi, K.Y. and No, H.C. (1995). Experimental Studies of Flooding in nealy Horizontal Pipes. *Int. J. Multiphase Flow*, Vol. 21, p 419-436.

Chung, K. S., C. P. Liu, C. L. Tien (1980). Flooding in Two-phase counter-current flows – II: Experimental Investigation. *PhysicoChemical Hydrodynamics*, Vol. 1, p209-220.

Deendarlianto, Ousaka, A., Kariyasaki, A., Fukano, T. and Konishi, M. (2004). The effects of surface tension on the flow pattern and counter-current flow limitation (CCFL) in gas-liquid two-phase flow in an inclined pipe. *Japanese Journal of Multiphase Flow*, Vol. 18, p337-350.

Fletcher, D, (2005). ISL Inc., email to K. Vierow.

Gauntt, R. O. et al., MELCOR Computer Code Manuals, Vol. 2: Reference Manuals, Version 1.8.6, Prepared by Sandia National Laboratories for the U.S. Nuclear Regulatory Commission, Office of Nuclear Regulatory Research, NUREG/CR-6119, Vol. 2, Rev. 3, SAND 2005-5713, Sept. 2005.

Girard, R. and Chang J.S. (1992). Reflux condensation phenomena in single vertical tubes. International Journal of Heat Mass Transfer, Vol.35, p2203-2218.

Hewitt, G. F. (1996). In search of two-phase flow. *Transactions of the ASME, Journal of Heat Transfer*, Vol. 118, p518-27.

Hogan, K., Vierow, K. (2008). A New Drift Flux-Based Approach to Predict Flooding. *U.S. Japan Seminar on Two-Phase Flow Dynamics*, Santa Barbara, CA.

Idaho National Engineering and Environmental Laboratory (1999). RELAP5/MOD3 Code Manual Vol. I: Code Structure, System Models, and Solution Methods (NUREG /CR-5535, Vol. I).

Jayanti, S., Tokarz, A. and Hewitt, G.F. (1996). Theoretical investigation of the diameter effect on flooding in countercurrent flow. *International Journal of Multiphase Flow*, Vol. 22, p307-324.

Jeong, J.H. and No, H.C. (1996). Experimental Study of the Effect of Pipe Length and Pipe-end Geometry on Flooding. *Int. J. Multiphase Flow*, Vol. 22, p 499-514.

Lacey, C. E. and Dukler, A. E. (1994). Flooding in vertical tubes--II. A film model for entry region flooding. *Int. J. Multiphase Flow*, Vol.20, pp. 235-247.

Lee, S.C. and Bankoff, S.G. (1983). Stability of steam-water countercurrent flow in an inclined channel. *Journal of Heat Transfer,* Vol.105, p713-718.

Liao, Y. and Vierow, K. (2005). MELCOR Modeling of Creep Rupture in Steam Generator Tubes, *Nuclear Technology*, Vol. 152, No. 3 p302-313.

Liao, Y. and Vierow, K. (2006). Optimum Channel Inclination for Gas Venting Under Countercurrent Flow Limiations. Proc. of ICONE-14 International Conference on Nuclear Engineering. Paper ICONE14-89665, Miami, FL.

Los Alamos National Laboratory and Pennsylvania State University (2000). TRAC-M /FORTRAN 90 (V 3.0) Theory Manual (LA-UR-00-910).

McQuillan, K.W. and Whalley, P.B. (1985). A comparison between flooding correlations and experimental flooding data for gas-liquid flow in vertical circular tubes. *Chemical Engineering Science*, Vol.40, p1425-1440.

Mouza, A.A., Paras, S.V., and Karabelas, A.J. (2003). Incipient flooding in inclined tubes of small diameter. *International Journal of Multiphase Flow*, Vol.29, p1395–1412.

Rothe, P. H., C. J. Crowley, (1978). Scaling Pressure and Subcooling for Countercurrent Flow, prepared by Creare, Inc. for U. S. Nuclear Regulatory Commission, NUREG/CR-0464, CREARE-TN-285.

Solmos, M. A. (2008). An Experimental Investigation of the Countercurrent Flow Limitation. M.S. Thesis, Texas A&M University, College Station, TX.

Takeuchi, K., Young, M.Y., and Gagnon, A.F. (1999). Flooding in the pressurizer surge line of AP600 plant and analyses of APEX data. *Nuclear Engineering and Design,* Vol.192, p45–58.

Vierow, K., T. Nagae, T. Wu, "Experimental Investigation of Reflux Condensation Heat Transfer in PWR Steam Generator Tubes in the Presence of Noncondensible Gases", 10th International Topical Meeting on Nuclear Reactor Thermal Hydraulics (NURETH-10), Seoul, Korea, Oct. 2003.

Vierow, K., Liao, Y., Johnson, J., Kenton, M. and Gauntt, R. (2004). Severe Accident Analysis of a PWR Station Blackout with the MELCOR, MAAP4 and SCDAP/RELAP5 Codes, *Nuclear Engineering and Design*, Vol. 234, p129-145.

Vijayan, M., Jayanti, S. and Balakrishnan, A.R. (2001). Effect of tube diameter on flooding. *International Journal of Multiphase Flow*, Vol. 27, p 797-816.

Wallis, G.B. (1969). One-dimensional Two-phase Flow. New York: McGraw-Hill.

Wallis, G. B., D. C. deSieyes, R. J. Rosselli, J. Lacombe, (1980). Countercurrent Annular Flow Regimes for Steam and Subcooled Water in a Vertical Tube. Prepared by Dartmouth College for Electric Power Research Institute, NP-1336, Research Project 443-2.

Wallis, G. B. and Makkencherry, S. (1974). The Hanging Film Phenomenon in Vertical Annular Two-Phase Flow. *Transactions of the ASME - Jnl. Fluids Engineering*, p297-298.

Wongwises, S. (1998). Effect of inclination angles and upper end conditions on the countercurrent flow limitation in straight circular pipes. *Int. Commun. Heat Mass Transfer*, Vol. 25, p117–125.

Wu, T. and Vierow, K. (2006). Experimental Study of Steam Horizontal In-Tube in the Condensation in the Presence of a Noncondensable Gas. *International Journal of Heat and Mass Transfer*, Vol. 49, p2491-2501.

Zapke, A. and Kroger, D.G. (1996). The Influence of Fluid Properties and Inlet Geometry on Flooding in Vertical and Inclined Tubes. *Int. J. Multiphase Flow*, Vol. 22, No. 3, p 461-472.

Zapke, K. and Kroger, D.G. (2000). Countercurrent gas-liquid flow in inclined and vertical ducts - II: The validity of the Froude-Ohnesorge number correlation for flooding. *International Journal of Multiphase Flow*, Vol. 26, p1457-1468.